

**Thermal-Fluid Control via
Finite-Dimensional Approximation**

Ajit R. Shenoy
Eugene M. Cliff
Matthias Heinkenschloss
Interdisciplinary Center for Applied Mathematics
and Department of Mathematics
Virginia Polytechnic Institute and State University

ICAM REPORT 96-04-01

AIAA Paper 96-1910
31st AIAA Thermophysics Conference
June 17-20, 1996 / New Orleans, LA

Interdisciplinary Center for Applied Mathematics
Virginia Polytechnic Institute and State University
Blacksburg, VA 24061

April, 1996

THERMAL-FLUID CONTROL VIA FINITE-DIMENSIONAL APPROXIMATION

Ajit R. Shenoy*

Eugene M. Cliff†

Matthias Heinkenschloss‡

Interdisciplinary Center for Applied Mathematics

Virginia Tech

Blacksburg, Virginia 24061

Abstract

We formulate a thermal-fluid control problem wherein the physics are described by a system of partial differential equations and the control enters through a thermal boundary condition. A finite-element approximation is used to transcribe this to a finite-dimensional Quadratic Programming problem. The finite-dimensional problem displays an expected sparsity pattern in the Jacobian of the constraints and the Hessian of the cost function. Three versions of the QP problem are considered—these differ in their treatment of certain control bounds. Numerical studies show that variants which faithfully reflect the structure of control bounds in the infinite-dimensional problem lead to well-behaved QP solutions, while variants that do not are troublesome for the QP algorithm. It is somewhat surprising that this behavior is apparent even when the finite-element grid is relatively coarse.

1. Introduction

Given below is a coupled solid-fluid temperature control problem, as described by Gunzburger and Lee.¹ We have the governing equations representing the 2-dimensional flow of a fluid within a solid container and the energy/heat transfer involved. The domain Ω in R^2 consists of the fluid subdomain Ω_2 , and the solid subdomain Ω_1 , separated by an interface Γ_w , with the result that $\Omega = \Omega_1 \cup \Omega_2 \cup \Gamma_w$ (see Figure 1). The solid region is bounded by $\Gamma_1 \cup \Gamma_2 \cup \Gamma_3 \cup \Gamma_w$ and the fluid flow occupies a domain Ω_2 having a boundary $\Gamma_c \cup \Gamma_o \cup \Gamma_w \cup \Gamma_4$. We have an

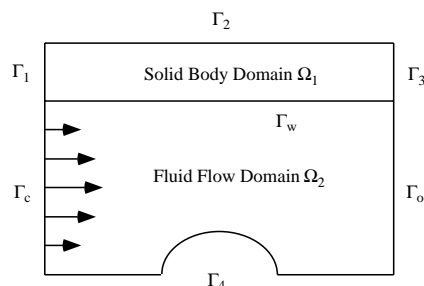


Figure 1: The Domain Ω

inflow boundary Γ_c , an outflow boundary Γ_o , and a solid wall Γ_w . The geometry of all these boundary segments is prescribed.

The problem is motivated by the desire to remove temperature peaks, *i.e.*, “hot spots” along the bounding surfaces of containers of fluid flows. We desire, then, to regulate the temperature along Γ_w or a portion $\Gamma_\sigma \subset \Gamma_w$. Control is to be effected by heating and cooling along the inflow boundary Γ_c . The heat equation for the solid domain is coupled to the energy equation for the fluid flow. Heat sources may be located in the solid body, the fluid, or both. The flow is assumed to be stationary, incompressible and convection driven, so that buoyancy effects can be neglected, and thus temperature effects on the mechanical properties of the flow, *i.e.*, the velocity and pressure, are negligible. The inflow velocity is prescribed, and “reasonable” boundary conditions may be imposed on the outflow boundary, Γ_o .

As a result of our assumptions about the flow, the state variables, *i.e.*, the velocity \mathbf{u} , pressure p , temperature T , and control g are required to satisfy the Navier-Stokes

*Graduate Student, Aerospace Engg. Dept., Student Member, AIAA

†Reynolds Metal Professor, Aerospace Engg. Dept., Associate Fellow, AIAA

‡Assistant Professor, Mathematics Department

equations

$$-\nu \Delta \mathbf{u} + (\mathbf{u} \cdot \nabla) \mathbf{u} + \nabla p = \mathbf{f} \quad \text{in } \Omega_2, \quad (1)$$

the incompressibility constraint

$$\operatorname{div} \mathbf{u} = 0 \quad \text{in } \Omega_2, \quad (2)$$

and, for simplicity, the boundary condition

$$\mathbf{u} = \mathbf{h} \quad \text{on } \Gamma_c, \quad (3)$$

$$\mathbf{u} = \mathbf{0} \quad \text{on } \Gamma_w \cup \Gamma_4, \quad (4)$$

$$\frac{\partial \mathbf{u}}{\partial n} = \mathbf{0} \quad \text{on } \Gamma_o, \quad (5)$$

and the energy equations

$$-\kappa_1 \Delta T = \bar{Q}_1 \quad \text{in } \Omega_1, \quad (6)$$

$$-\kappa_2 \Delta T + (\mathbf{u} \cdot \nabla) T = \bar{Q}_2 + 2\mu(\nabla \mathbf{u} + \nabla \mathbf{u}^T) : (\nabla \mathbf{u} + \nabla \mathbf{u}^T) \quad \text{in } \Omega_2, \quad (7)$$

with the boundary conditions

$$T = g \quad \text{on } \Gamma_c, \quad (8)$$

$$\frac{\partial T}{\partial n} = 0 \quad \text{on } \Gamma_1 \cup \Gamma_2 \cup \Gamma_3 \cup \Gamma_4 \cup \Gamma_o. \quad (9)$$

The data functions \mathbf{f} , \mathbf{h} , \bar{Q}_1 and \bar{Q}_2 are assumed to be known. The constant ν is the kinematic viscosity coefficient of the fluid, and the constants κ_1 , κ_2 and μ depend on the thermal conductivity coefficient, density, specific heat at constant volume, and viscosity coefficient of the fluid; see Serrin⁴ for details.

Note that as a result of our assumptions about the flow, the mechanical equations (1)–(5) uncouple from the thermal equations (6)–(9). Indeed, (1)–(5) may be solved for \mathbf{u} and p without regard of the temperature T . Thus, in the present context, the velocity field \mathbf{u} , which is determined by solving (1)–(5), merely acts as a coefficient function and in the source term in (7).

Our goal is to find, for a given velocity field \mathbf{u} , a boundary control g such that on Γ_o the temperature field T given by (6)–(9) is as close to the desired temperature $T_d(\cdot)$ as possible. We measure closeness in the least squares sense. This leads to the following objective function:

$$\begin{aligned} \mathcal{J}(T, g) &= \frac{1}{2} \int_{\Gamma_o} |T - T_d|^2 d\Gamma \\ &+ \frac{\delta}{2} \int_{\Gamma_c} (|g|^2 + |\nabla_s g|^2) d\Gamma. \end{aligned} \quad (10)$$

Here ∇_s denotes the surface gradient operator. The non-negative parameter δ acts as a regularization parameter

and can be used to change the relative importance of the two terms appearing in the definition of \mathcal{J} .

2. The Optimal Control Problems

The first optimal control problem investigated in this paper is given by

$$\begin{aligned} &\text{Minimize } \mathcal{J}(T, g) \\ &\text{subject to the equations (6)–(9).} \end{aligned} \quad (\text{P1})$$

Here we assume that $\delta > 0$. This control problem has been studied by Gunzburger and Lee.¹ They have shown that if the flow satisfies

$$\begin{aligned} \mathbf{u} \cdot \mathbf{n} &= 0 \quad \text{on } \Gamma_w \cup \Gamma_4, \\ \mathbf{u} \cdot \mathbf{n} &\geq 0 \quad \text{on } \Gamma_o, \end{aligned} \quad (11)$$

then the state equation (6)–(9) has a unique solution $T \in H^1(\Omega)$ for all $g \in W(\Gamma_c)$, $\bar{Q}_1 \in H^{-1}(\Omega_1)$, $\bar{Q}_2 \in H^{-1}(\Omega_2)$, which depends continuously on these data. The function spaces are given by

$$H^1(\Omega) = \{v \mid v \in L^2(\Omega), \frac{\partial}{\partial x_j} v \in L^2(\Omega), j = 1, 2\}$$

and

$$W(\Gamma_c) = \{g \in H^1(\Gamma_c) \mid g = 0 \text{ at } \bar{\Gamma}_c \cap \bar{\Gamma}_1\}.$$

See *e.g.*, Adams² and Ciarlet³ for more details on these Sobolev spaces. Under these conditions, the optimal control problem (P1) admits a unique solution. The presence of the penalty term $\frac{\delta}{2} \int_{\Gamma_c} (|g|^2 + |\nabla_s g|^2) d\Gamma$, $\delta > 0$, is crucial in the existence and uniqueness proof, since it implicitly imposes a bound on the controls. While the optimal control problem with the penalized objective function is relatively easy to solve, the penalty term does not allow a direct manipulation of the bound on the control. Therefore, it is often desirable to replace the penalty term in (P1) by a constraint on the controls. The immediate choice $|g(x)| \leq \bar{g}$ for all $x \in \Gamma_c$ is not feasible in our framework, since it does not guarantee the boundary value to be in $H^{1/2}(\Gamma_c)$, a condition necessary to ensure solvability of the state equation (6)–(9) in $H^1(\Omega)$. We do not consider possible relaxations of the meaning of a solution to (6)–(9). Instead, we impose a bound on the control and its derivative, $|g(x)| \leq \bar{g}^0$, $|g'(x)| \leq \bar{g}^1$. Together with $g = 0$ at $\bar{\Gamma}_c \cap \bar{\Gamma}_1$ this implies $g \in W(\Gamma_c)$. This leads to the following optimal control problem:

$$\begin{aligned} &\text{Minimize } \mathcal{J}(T, g) \\ &\text{subject to the equations (6)–(9) and} \\ &\text{subject to } |g(x)| \leq \bar{g}^0, \quad \forall x \in \Gamma_c, \\ &|g'(x)| \leq \bar{g}^1, \quad \forall x \in \Gamma_c. \end{aligned} \quad (\text{P2})$$

In (13) we use ξ_0 to denote the local coordinate for the i th element at $x = x_0$, where x_0 represents the x-coordinate at the inlet to the duct, and η_f to denote the local coordinate for the i th element at $y = y_f$, where y_f is the y-coordinate at the fluid-solid interface. Note, that $T_i^d(\xi)$ is the localized representation of the desired temperature distribution, $T_d(\cdot)$, on the fluid-solid interface, Γ_σ , for the i th element.

Consider the first term in the objective function. For any element within E_w , the contribution to the objective function can be seen to be

$$\mathcal{J}_{1i}^h = \frac{l_{xi}}{2} \sum_{j=1}^6 \int_0^1 (\theta_{i_j} \phi_j(\xi, \eta_f) - T_i^d(\xi))^2 d\xi \quad (14)$$

This simplifies to,

$$\mathcal{J}_{1i}^h = \frac{l_{xi}}{2} \sum_{j=1}^6 (C_{2j} \theta_{i_j}^2 + C_{1j} \theta_{i_j} + C_{0j})$$

where, C_{0j} , C_{1j} and C_{2j} are constants, given by

$$\begin{aligned} C_{2j} &= \int_0^1 \phi_j(\xi, \eta_f)^2 d\xi, \\ C_{1j} &= -2 \int_0^1 T_i^d(\xi) \phi_j(\xi, \eta_f)^2 d\xi, \quad \text{and} \\ C_{0j} &= \int_0^1 T_i^d(\xi)^2 d\xi, \end{aligned}$$

respectively. The above term (14) is a perfect quadratic expression involving θ^i . We can show, similarly, that the contributions from the elements within E_c , for the penalty terms in the objective function, are also quadratic expressions. We have linear constraints comprising the discretized governing equations, and bounds on the variables, if any. Thus, the resulting problem can be seen to be a quadratic programming problem.

Now we are able to formulate the three discrete optimal control problems that we study in this paper. The first discrete optimal control problem corresponds to (P1) and is given by

$$\begin{aligned} \text{Minimize} \quad & \mathcal{J}^h(\vec{\theta}, \vec{g}) \\ \text{s.t.} \quad & \mathbf{A}\vec{\theta} = \mathbf{b}(\vec{g}), \end{aligned} \quad (\text{DP1})$$

where $\delta > 0$. Under the condition (11) on \mathbf{u} , the matrix \mathbf{A} can shown to be positive definite and it is not hard to show that the quadratic programming problem (DP1) has a unique solution. The fact that the penalty parameter δ is positive is also important in the discrete case. Gunzburger and Lee¹ have studied the convergence of the solution to the discretized problems (DP1) to the solution to (P1) as $h \rightarrow 0$.

In the discrete framework it is tempting to replace the penalty term by bound constraints. This leads to the problem

$$\begin{aligned} \text{Minimize} \quad & \mathcal{J}^h(\vec{\theta}, \vec{g}) \\ \text{s.t.} \quad & \mathbf{A}\vec{\theta} = \mathbf{b}(\vec{g}) \\ & |\vec{g}| \leq \vec{g}^0, \end{aligned} \quad (\text{DP2})$$

where we assume that $\delta = 0$. Here $|\vec{g}| \leq \vec{g}^0$ is understood component wise. Using standard arguments, it can be seen that the problem (DP2) has a solution. Notice, that, as discussed previously, the infinite dimensional version of the discrete problem (DP2) may not have a solution. To understand (DP2), we use inverse inequalities. It is well known, see *e.g.* Ciarlet,³ that for quasi-uniform finite element discretizations there exists a constant c independent of h such that

$$\max_{\Gamma_c} |g'_h(y)| \leq \frac{c}{h} \max_{\Gamma_c} |g_h(y)|. \quad (15)$$

Here g_h denotes the piecewise quadratic function corresponding to the vector of coefficients \vec{g} . Due to the inverse inequality (15) the bound $|\vec{g}| \leq \vec{g}^0$ on the coefficients implies bounds on $\max_{\Gamma_c} |g_h(y)|$ and on $\max_{\Gamma_c} |g'_h(y)|$. However, these bounds depend on h and the second bound will grow towards infinity as h goes to zero. In fact, if i_1, i_2, i_3 are the indices of the nodes on the edge i , then the local control is given by

$$\begin{aligned} g_{hi}(y) &= g_{i_1} \frac{(y-y_{i_2})(y-y_{i_3})}{(y_{i_1}-y_{i_2})(y_{i_1}-y_{i_3})} \\ &+ g_{i_2} \frac{(y-y_{i_1})(y-y_{i_3})}{(y_{i_2}-y_{i_1})(y_{i_2}-y_{i_3})} \\ &+ g_{i_3} \frac{(y-y_{i_1})(y-y_{i_2})}{(y_{i_3}-y_{i_1})(y_{i_3}-y_{i_2})}. \end{aligned} \quad (16)$$

Thus,

$$|g_h(y)| \leq c_0 \|\vec{g}\|_\infty \quad \forall y \in \Gamma_c$$

for some c_0 independent of h . By the inverse inequality,

$$|g'_h(y)| \leq \frac{c_1}{h} \|\vec{g}\|_\infty \quad \forall y \in \Gamma_c$$

for some c_1 independent of h . Hence, for coarse discretizations, *i.e.* large h , the bound $|\vec{g}| \leq \vec{g}^0$ should be sufficient, but as the mesh is refined, *i.e.*, h is decreased, the bound $|\vec{g}| \leq \vec{g}^0$ must be tightened to guarantee a reasonable bound on $|g'_h(y)|$. This behavior is typical if there is no well-posed infinite dimensional problem formulation corresponding to the discrete problem formulations. In this case, even though the discrete problem formulation may be well posed for arbitrary fine but fixed discretization levels, there is no convergence of the solutions for the discrete problems as h tends to zero. This will be demonstrated by our numerical results. Moreover, it

is important to notice, that this effect is not only of theoretical interest, but as the discretizations are refined, optimization methods applied to solve (DP2) will perform extremely poorly. We will return to this issue later.

In view of the preceding discussion, we want to add a constraint to (DP2) which bounds the derivative of g_h . Using the local control (16) on the edge i , we find that

$$g'_{hi}(y) = g_{i_1} \frac{2y - y_{i_2} - y_{i_3}}{l_{yi}/2} + g_{i_2} \frac{2y - y_{i_1} - y_{i_3}}{-l_{yi}/4} + g_{i_3} \frac{2y - y_{i_1} - y_{i_2}}{l_{yi}/2}.$$

Here we assume that y_{i_1}, y_{i_3} are the endpoints of the edge and y_{i_2} is the midpoint and we used the fact that $|y_{i_1} - y_{i_3}| = l_{yi}$. Since $g'_{hi}(y)$ is linear, $|g'_{hi}(y)| \leq \bar{g}^1$ if and only if $|g'_{hi}(y_{i_1})| \leq \bar{g}^1$ and $|g'_{hi}(y_{i_3})| \leq \bar{g}^1$. This leads to

$$\begin{aligned} |g_{i_1} \frac{2y_{i_1} - y_{i_2} - y_{i_3}}{l_{yi}/2} + g_{i_2} \frac{y_{i_1} - y_{i_3}}{-l_{yi}/4} \\ + g_{i_3} \frac{2y_{i_1} - y_{i_1} - y_{i_2}}{l_{yi}/2}| &\leq \bar{g}^1, \\ |g_{i_1} \frac{2y_{i_3} - y_{i_2} - y_{i_3}}{l_{yi}/2} + g_{i_2} \frac{y_{i_3} - y_{i_1}}{-l_{yi}/4} \\ + g_{i_3} \frac{2y_{i_3} - y_{i_1} - y_{i_2}}{l_{yi}/2}| &\leq \bar{g}^1. \end{aligned}$$

Using the fact that $|y_{i_1} - y_{i_3}| = l_{yi}$ we arrive at the inequalities

$$\begin{aligned} \frac{1}{l_{yi}} | -3g_{i_1} + 4g_{i_2} - g_{i_3} | &\leq \bar{g}^1, \\ \frac{1}{l_{yi}} | -g_{i_1} + 4g_{i_2} - g_{i_3} | &\leq \bar{g}^1. \end{aligned}$$

If we impose this for all edges on the control boundary Γ_c , then we arrive at the inequalities

$$|\mathbf{T}\vec{g}| \leq \bar{g}^1,$$

where $\mathbf{T} \in \mathbb{R}^{2N_g \times N_g}$ is composed of two square tridiagonal matrices. This leads to the following problem:

$$\begin{aligned} \text{Minimize } & \mathcal{J}^h(\vec{\theta}, \vec{g}) \\ \text{s.t. } & \mathbf{A}\vec{\theta} = \mathbf{b}(\vec{g}) \\ & |\vec{g}| \leq \bar{g}^0 \\ & |\mathbf{T}\vec{g}| \leq \bar{g}^1. \end{aligned} \quad (\text{DP3})$$

Again, (DP3) is well posed. Moreover, it corresponds to the infinite dimensional problem (P2).

4. Numerical Results

For the solution of the optimal control problems (DP1), (DP2), (DP3) any method for the solution of quadratic programming problems can be used. We applied a sparse optimization code developed by Betts.⁶ Betts' code is a sequential quadratic programming (SQP) based method for the solution of nonlinear problems. Therefore it is designed to solve much more general problems and most of its features are not needed when it is applied to solve (DP1), (DP2), or (DP3). However, since this research was performed in a larger context, including nonlinear phenomena and since the speed of convergence of the optimizer is not the focus of this paper, we used this package.

As a test problem we have chosen one of the problems considered by Gunzburger and Lee. The domain Ω is the unit square $(0, 1) \times (0, 1) \subset \mathbb{R}^2$ with sub-domains $\Omega_1 = (0, 1) \times (0.75, 1)$ and $\Omega_2 = (0, 1) \times (0, 0.75)$. Thus, the fluid–solid interface is the line $y_{fs} = 0.75$. As the line on which the temperature is to be matched we choose $\Gamma_\sigma = (0.075, 1) \times \{0.75\} \subset \Gamma_w = (0, 1) \times \{0.75\}$. The control boundary is $\Gamma_c = \{0\} \times (0, 0.75)$. (See Figure 1 without the bump on the bottom boundary).

We consider the following problem

$$-\Delta T = 6.0 \quad \text{on } \Omega_1, \quad (17)$$

$$-2\Delta T + (\mathbf{u} \cdot \nabla)T = 0 \quad \text{on } \Omega_2, \quad (18)$$

$$T = 1 + \hat{g} \quad \text{on } \Gamma_c, \quad (19)$$

$$\frac{\partial T}{\partial n} = 0 \quad \text{on } \partial\Omega \setminus \Gamma_c, \quad (20)$$

where the velocity \mathbf{u} is the solution of the Navier-Stokes equations

$$-\Delta \mathbf{u} + (\mathbf{u} \cdot \nabla)\mathbf{u} + \nabla p = \mathbf{0} \quad \text{in } \Omega_2, \quad (21)$$

the incompressibility constraint

$$\text{div } \mathbf{u} = 0 \quad \text{in } \Omega_2, \quad (22)$$

and the boundary condition

$$\mathbf{u} = \mathbf{h} \quad \text{on } \Gamma_c, \quad (23)$$

$$\mathbf{u} = \mathbf{0} \quad \text{on } \Gamma_w \cup \Gamma_4, \quad (24)$$

$$\frac{\partial u_1}{\partial n} = 0 \quad \text{and} \quad u_2 = 0 \quad \text{on } \Gamma_\sigma, \quad (25)$$

where $\mathbf{u} = (u_1, u_2)$ and $\mathbf{h} = (1.5y - 2y^2, 0)$. We have a simple solution, $\mathbf{u} = (1.5y - 2y^2, 0)$, for the above Navier-Stokes problem.

In keeping with the results that Lee and Gunzburger obtained, we also impose an additional condition, $\hat{g}(y_{f_s}) = 0$, which in terms of the finite element problem corresponds to the condition, $g_{n_g} = 1$. All cases were started from an initial point, corresponding to the solution to equations (17)–(20), with $g = 0$ in equation (19). This problem is referred to as the uncontrolled problem, and its numerical solution is shown in Figure 3 and Figure 4. The solution to the uncontrolled problem is used as an initial guess for the optimizer.

It can be seen from the above mentioned figures that the temperature is above 2.0 on $(0.3, 1) \times \{0.75\}$ and even higher in the domain $(0.3, 1) \times (0.75, 1)$. We try to regulate the temperature along Γ_σ . Any reasonable temperature distribution may be chosen. Following Gunzburger and Lee, we have chosen to target $T_d = 1.2$ on Γ_σ . Thus, we have

$$\mathcal{J}(T, g) = \frac{1}{2} \int_{\Gamma_\sigma} |T - 1.2|^2 d\Gamma + \frac{1}{\delta} \int_{\Gamma_c} (|g - 1|^2 + |\nabla_s g|^2) d\Gamma. \quad (26)$$

Note that we penalize \hat{g} . Therefore, in the control $g = 1 + \hat{g}$ the penalty term is given by $\int_{\Gamma_c} (|g - 1|^2 + |\nabla_s g|^2) d\Gamma$.

First, we duplicate some of the results computed by Gunzburger and Lee,¹ *i.e.*, we solve (DP1) with data and the modifications for g outlined above. We use the penalty parameters $\delta = 1$ and $\delta = 6 \times 10^{-5}$. The costs computed for a 13×13 grid are indicated in Table 1.

Table 1: Objective Function Values (13×13 Grid).

	$\ T^h - 1.2\ _{0, \Gamma_\sigma}^2$	$\ g^h\ _{1, \Gamma_c}^2$	$\mathcal{J}^h(T, g)$
uncontrolled	1.1548	0	0.5774
$\delta = 2$	1.0751	0.0196	0.5571
$\delta = 6 \times 10^{-5}$	0.00155	66.90	0.0028

As can be expected, for $\delta = 2$, where we place a high weight on the size of the control, the optimal solution does not exhibit a significantly large change in the control effort. The numerical results for this case are shown in Figures 5 and 6 through a temperature surface plot, and a contour plot, respectively.

When the relative weight on the penalty term is reduced, $\delta = 6 \times 10^{-5}$, we find that the control exhibits much more dynamical behavior. Results for this case are shown in Figures 7 and 8 through temperature surface and contour plots, respectively.

The temperature distributions at the inlet to the duct, obtained in the two cases, are plotted in Figure 9. A comparison of the temperature distributions generated at the solid-fluid interface for the two cases is shown in Figure 10. As would be expected, the optimal control does a

much better job at tracking the desired temperature profile for the second case.

We remark that the results we have obtained do not agree with those reported by Lee and Gunzburger. In fact, there seem to be some inconsistencies in their results. Personal communication with the authors indicated that they have used some scaling to accelerate convergence. This leads us to believe that they have reported inconsistent values of δ for the cases they have shown.

The costs for various grid sizes with $\delta = 6 \times 10^{-5}$ are shown in Table 3. Figures 11 and 12 show comparisons of the results obtained for each case, in terms of the optimal control distribution obtained and the temperature distribution at the interface generated, respectively.

Table 2: Grid Sizes.

grid size	N_n	N_g
7×7	169	8
13×13	625	18
25×25	2401	36
33×33	4225	48

Table 3: Grid Convergence Study for Problem (DP1) with $\delta = 6 \times 10^{-5}$.

grid size	$\ T - 1.2\ _{0, \Gamma_\sigma}^2$	$\ g - 1\ _{1, \Gamma_c}^2$	$\mathcal{J}^h(T, g)$
7×7	1.47×10^{-3}	67.66	2.76×10^{-1}
13×13	1.55×10^{-3}	66.90	2.78×10^{-1}
25×25	1.72×10^{-3}	74.47	3.10×10^{-1}
33×33	1.60×10^{-3}	69.28	2.88×10^{-1}

Next we consider the optimal control problem (DP2) with explicit bounds on the control variables and with $\delta = 0$. As we have shown earlier, the bounds on the coefficients of the discretized control impose a crude bound on ∇g^h which, however, depends on $1/h$. The lack of penalization of the control shows in the computed controls, and also in the performance of the optimizer. Unless a tight bound on \vec{g} is enforced, the optimizer performs rather poorly. This can be attributed to a lack of regularity of the solution. While the penalized problem (DP1) has a unique solution which converges to the solution of the corresponding infinite dimensional problem, such a convergence property does in general not hold for the solutions of (DP2). Compare Figures 11 and 17. For the penalized problem (DP1) the properties of the infinite dimensional problem, in particular the strict convexity of the infinite dimensional problem, determine the properties of the discretized problem (DP1). Since there is no well-posed infinite dimensional problem corresponding to (DP2), such a behavior can not be expected in this case. In fact, our results indicate the strict convexity of the problem (DP2) is related to the grid size h . The larger h , the more strictly convex the problem is, *i.e.* the larger

the eigenvalues of the Hessian projected onto the null-space of the active constraints.

The optimal control obtained for this case is shown in Figure 13. The ‘*’s and ‘o’'s indicate the positions of the nodes (and their temperature values) for the problem, using a 13×13 grid. The results show that most of the control nodes are at either of the two bounds. The algorithm seems to have trouble in determining the correct active set in this case. The problem worsens as the bounds are pushed out. The controls obtained for the cases when $|\bar{g}| \leq 4$ and $|\bar{g}| \leq 8$ are shown in Figures 14 and 15, respectively. These figures also confirm our previous analysis. If the bound on $|\bar{g}|$ becomes too large relative to h , then the derivative of g^h is essentially unbounded. This can be seen in Figures 13 to 15. As the bound on $|\bar{g}|$ is relaxed, the computed solution g^h tends to oscillate and the oscillations increase as the bound is further relaxed. It should also be noted that tight bounds on $|\bar{g}|$ seem to be necessary to guarantee that the function g^h roughly lies between the same bounds as the vector of coefficients \bar{g} . We also point out that the discretization of size 13×13 is not particularly fine. Therefore, the poor behavior at this rather coarse discretization level is somewhat surprising.

A comparison of the temperature distributions generated for the three cases, shown in Figure 16, indicates that the optimal solution does a better job at regulating the temperature as the bounds on the control are relaxed.

Finally, we consider the optimal control problem (DP3) with explicit bounds on the control variables and with $\delta = 0$. As expected, the numerical results are closer to those for the penalized formulation (DP1). Figures 18 to 20 show the computed controls for the constraints $|\bar{g}| \leq 4$, and $|\mathbf{T} \cdot \bar{g}| \leq 2, 20, 2000$, respectively. For reasonable bounds on the derivative ($|\mathbf{T} \cdot \bar{g}| \leq 2, 20$), the computed results are close to those for the penalized problem with appropriately chose penalty parameter δ . This shows very clearly in the match between computed and desired temperature (see Figures 10 and 21). However, similarities can also be observed in the computed controls. Compare the Figures 18 and 23, and the Figures 19 and 24. Of course, if the bound on the derivative is too large, then the results compare with those for problem (DP2). See *e.g.*, Figures 14 and 20. Generally, we can see a qualitative improvement, *i.e.*, less oscillatory behavior in the solutions of (DP3) compared with (DP2). Along with this we could also observed a much improved convergence behavior of the optimizer, due to the regularizing effect of the bound constraints, similar to the addition of a penalty term. As for the penalized problem (DP1), convergence of the computed controls as the grid is re-

finned can be observed. See Figure 22.

5. Conclusions

In this paper we have considered a thermal-fluid control problem wherein the physics are described by a system of partial differential equations and the control enters through a thermal boundary condition. A finite-element approximation was used to transcribe this to a finite-dimensional quadratic programming problem. Three versions of the discrete optimal control problem are considered. These differ in their treatment of certain control bounds. Two of these formulations correspond to infinite-dimensional optimal control problems. The numerical studies in this paper show that variants which faithfully reflect the structure of control bounds in the infinite-dimensional problem lead to well-behaved QP solutions, while variants that do not are troublesome for the QP algorithm. In the first case, the optimization algorithm behaves well and one can observe convergence of the discrete solutions as the grid is refined. In the second case when there is no corresponding infinite dimensional well-posed problem, however, the convergence behavior of the optimization algorithm deteriorates and the computed discretized solutions tend to oscillate as the discretization is refined. We have provided some explanations for this behavior. A more comprehensive mathematical analysis will be performed. We also plan to investigate other optimization algorithms, not available to us at the beginning of this research, such as interior point methods, *e.g.* Wright,⁷ for the linear case and SQP interior point methods, *e.g.* Dennis *et al*⁸ for the nonlinear case.

Acknowledgement

We would like to thank Dr. John Betts, Senior Principal Scientist at the Boeing Computer Services Research Division, for allowing us the use of his software, and for helping us with its implementation. This research was supported by the Air Force Office of Scientific Research under grant F49620-93-1-0280 and by the NSF under Grant DMS-9403699.

References

- [1] Gunzburger, Max D. and Lee, Hyung C., “Analysis, Approximation, and Computation of a Coupled Solid/Fluid Temperature Control Problem,” *Computational Methods in Applied Mechanics Engineering*, vol. 118, 1994, pp. 133–152

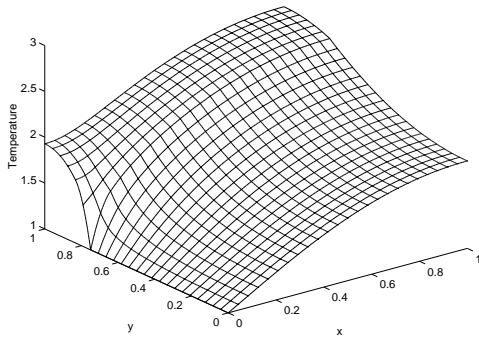


Figure 3: The temperature surface plot for the uncontrolled problem.

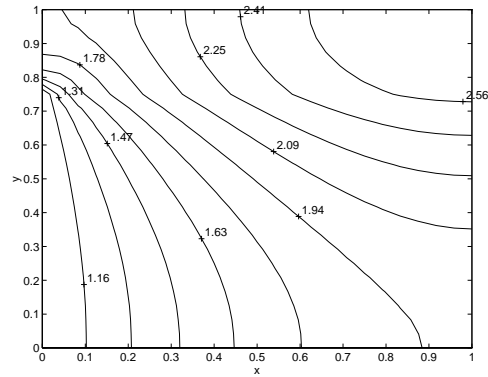


Figure 4: The temperature contour plot for the uncontrolled problem.

- [2] Adams, R. A., *Sobolev Spaces*, Academic Press, Orlando, San Diego, New-York, 1975.
- [3] Ciarlet, Philippe G., *The Finite Element Method for Elliptic Problems*, Studies in Mathematics and its Applied Problems, vol.4, (Ed. by J.L.Lions, G.Papanicolaou and R.T.Rockafellar), North-Holland, New York, 1979.
- [4] Serrin, J., *Mathematical principles of classical fluid mechanics*, *Handbuch der Physik VIII/1* (Ed. by S. Flügge and C. Truesdell), Springer, Berlin, 1959, pp. 125–263.
- [5] Zienkiewicz, O.C., *The Finite Element Method*, McGraw-Hill, London, 1977.
- [6] Betts, John T., “Software for Sparse Nonlinear Optimization,” Technical Document Series BCSTECH-93-054, Boeing Computer Services, December 1993.
- [7] Wright, M. H., “Interior point methods for constrained optimization”. In *Acta Numerica 1992*, ed. by A. Iserles, Cambridge University Press, Cambridge, New York, 1992, pp. 341–407.
- [8] Dennis, J. E., Heinkenschloss, M., and Vicente, L. N., “Trust–region interior–point algorithms for a class of nonlinear programming problems”, Technical Report 94–12–01, Interdisciplinary Center for Applied Mathematics, Virginia Tech, December 1994.

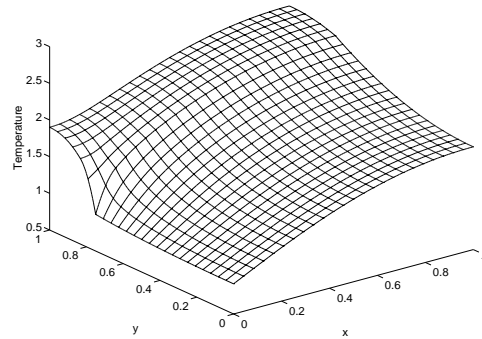


Figure 5: The temperature surface plot for Problem (DP1) with $\delta = 2$.

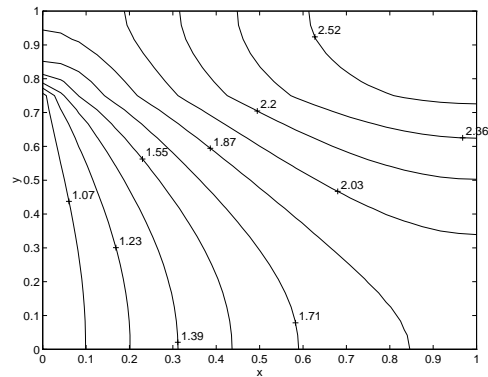


Figure 6: The temperature contour plot for Problem (DP1) with $\delta = 2$.

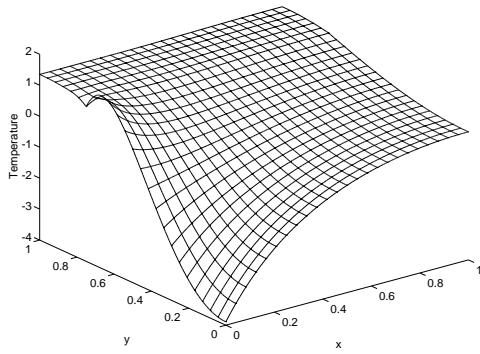


Figure 7: The temperature surface plot for Problem (DP1) with $\delta = 6 \times 10^{-5}$.

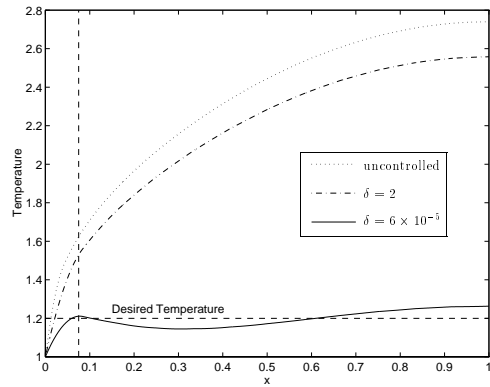


Figure 10: The Temperature Distributions on Γ_σ for Problem (DP1).

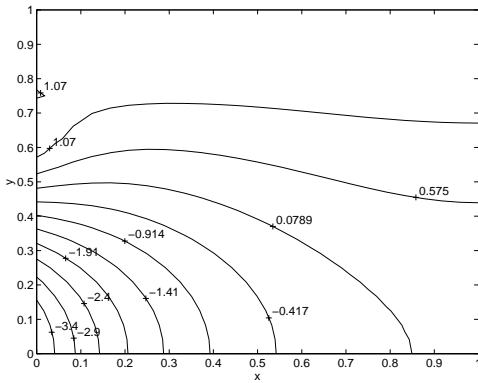


Figure 8: The temperature contour plot for Problem (DP1) with $\delta = 6 \times 10^{-5}$.

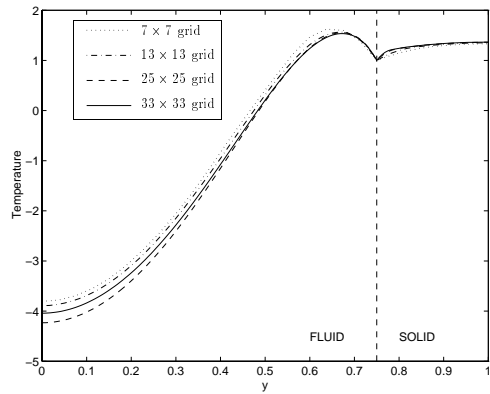


Figure 11: The Optimal Controls on Γ_c for Problem (DP1): Grid Study.

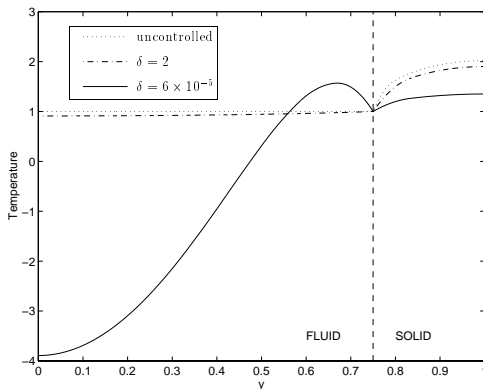


Figure 9: The Optimal Controls on Γ_c for Problem (DP1).

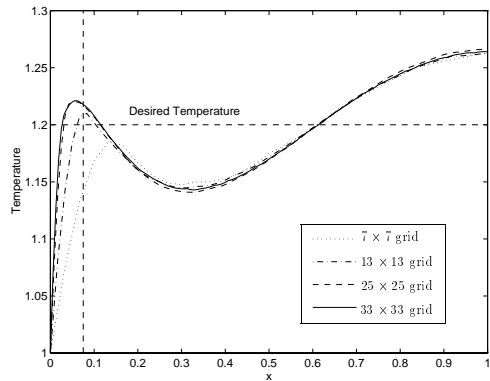


Figure 12: The Temperature Distributions on Γ_σ for Problem (DP1): Grid Study.

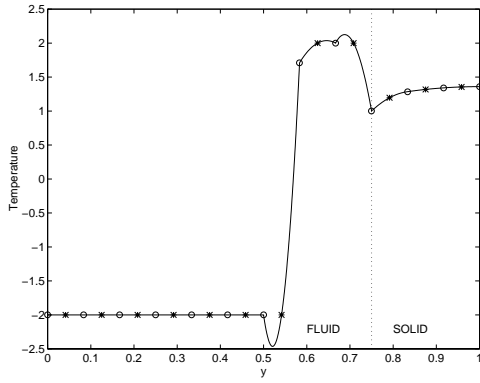


Figure 13: The Optimal Controls on Γ_c for Problem (DP2) with $|\vec{g}| \leq 2$.

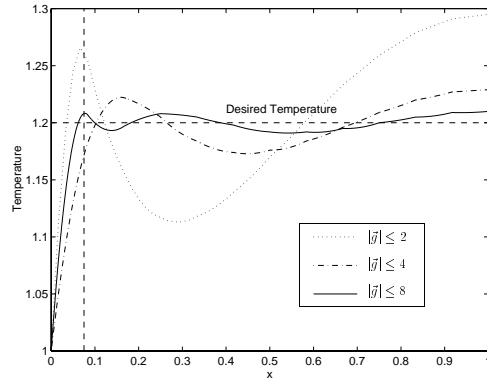


Figure 16: The Temperature Distributions on Γ_σ for Problem (DP2).

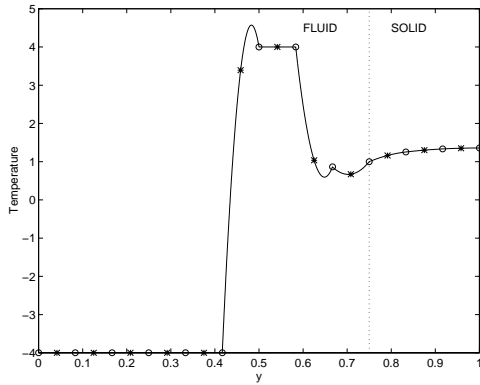


Figure 14: The Optimal Controls on Γ_c for Problem (DP2) with $|\vec{g}| \leq 4$.

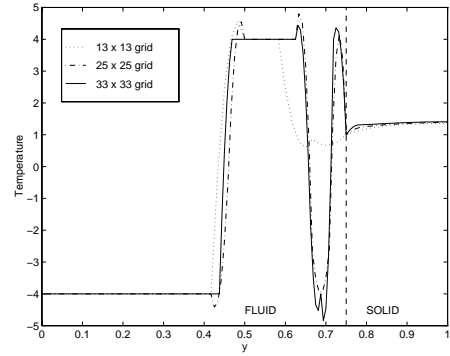


Figure 17: The Optimal Controls on Γ_c for Problem (DP2) with $|\vec{g}| \leq 4$: Grid Study

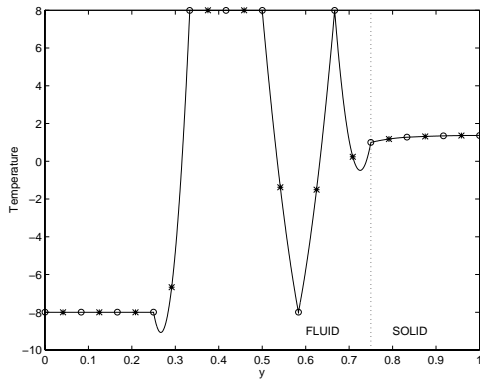


Figure 15: The Optimal Controls on Γ_c for Problem (DP2) with $|\vec{g}| \leq 8$.

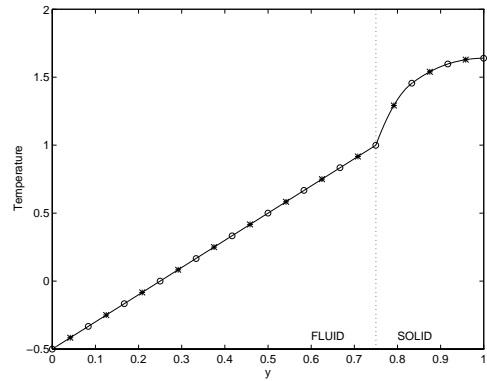


Figure 18: The Optimal Controls on Γ_c for Problem (DP3) with $|\vec{g}| \leq 4$, $|\mathbf{T} \cdot \vec{g}| \leq 2$.

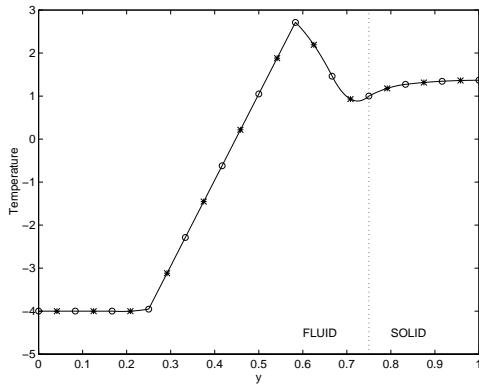


Figure 19: The Optimal Controls on Γ_c for Problem (DP3) with $|\vec{g}| \leq 4, |\mathbf{T} \cdot \vec{g}| \leq 20$.

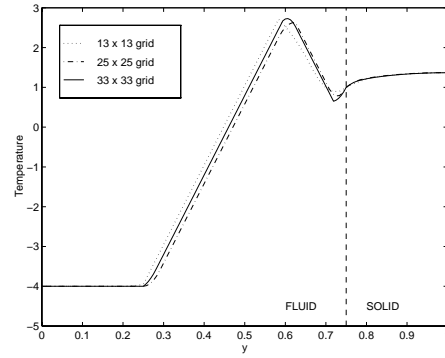


Figure 22: The Optimal Controls on Γ_c for Problem (DP3) with $|\vec{g}| \leq 4, |\mathbf{T} \cdot \vec{g}| \leq 20$: Grid Study.

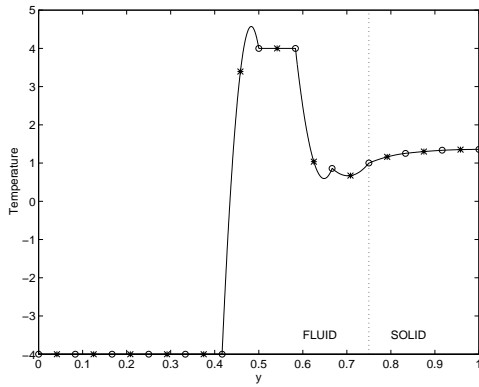


Figure 20: The Optimal Controls on Γ_c for Problem (DP3) with $|\vec{g}| \leq 4, |\mathbf{T} \cdot \vec{g}| \leq 2000$.

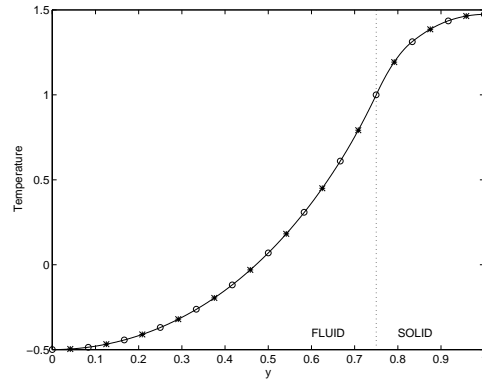


Figure 23: The Optimal Controls on Γ_c for Problem (DP1) with $\delta = 0.05$.

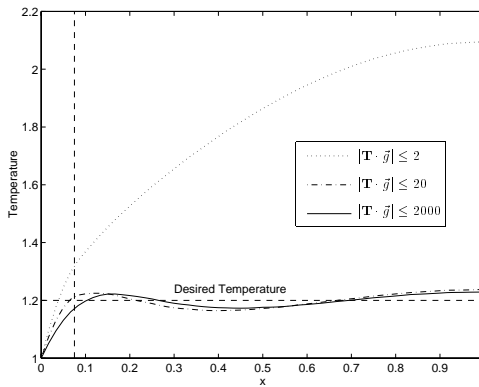


Figure 21: The Temperature Distributions on Γ_σ for Problem (DP3).

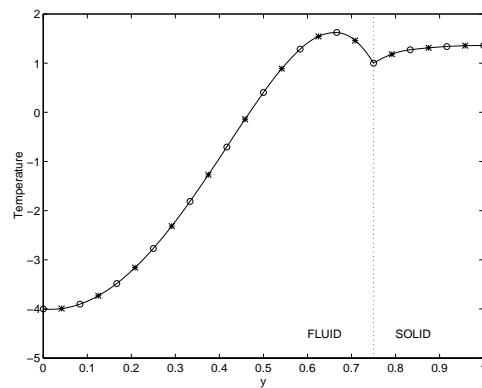


Figure 24: The Optimal Controls on Γ_c for Problem (DP1) with $\delta = 4 \times 10^{-5}$.